Computers and Mathematics with Applications 60 (2010) 2426–2432

Contents lists available at ScienceDirect

Computers and Mathematics with Applications

journal homepage: www.elsevier.com/locate/camwa

A novel automatic microcalcification detection technique using Tsallis entropy & a type II fuzzy index

Mohanalin *, Beenamol, Prem Kumar Kalra, Nirmal Kumar

Department of Electrical Engineering, IIT Kanpur, UP-208016, India

ARTICLE INFO

Article history:
Received 18 August 2009
Received in revised form 12 August 2010
Accepted 12 August 2010

Keywords:
Tsallis entropy
Type II fuzzy index
Shannon entropy
Mammograms
Microcalcification

ABSTRACT

This article investigates a novel automatic microcalcification detection method using a type II fuzzy index. The thresholding is performed using the Tsallis entropy characterized by another parameter 'q', which depends on the non-extensiveness of a mammogram. In previous studies, 'q' was calculated using the histogram distribution, which can lead to erroneous results when pectoral muscles are included. In this study, we have used a type II fuzzy index to find the optimal value of 'q'. The proposed approach has been tested on several mammograms. The results suggest that the proposed Tsallis entropy approach outperforms the two-dimensional non-fuzzy approach and the conventional Shannon entropy partition approach. Moreover, our thresholding technique is completely automatic, unlike the methods of previous related works. Without Tsallis entropy enhancement, detection of microcalcifications is meager: 80.21% Tps (true positives) with 8.1 Fps (false positives), whereas upon introduction of the Tsallis entropy, the results surge to 96.55% Tps with 0.4 Fps.

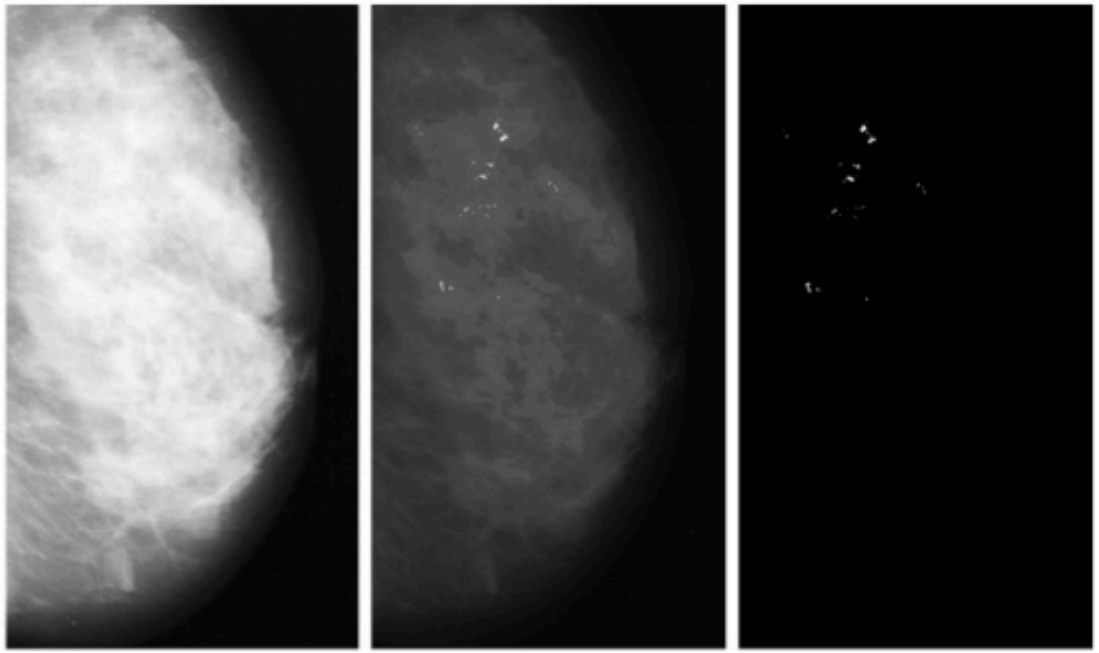

a b c

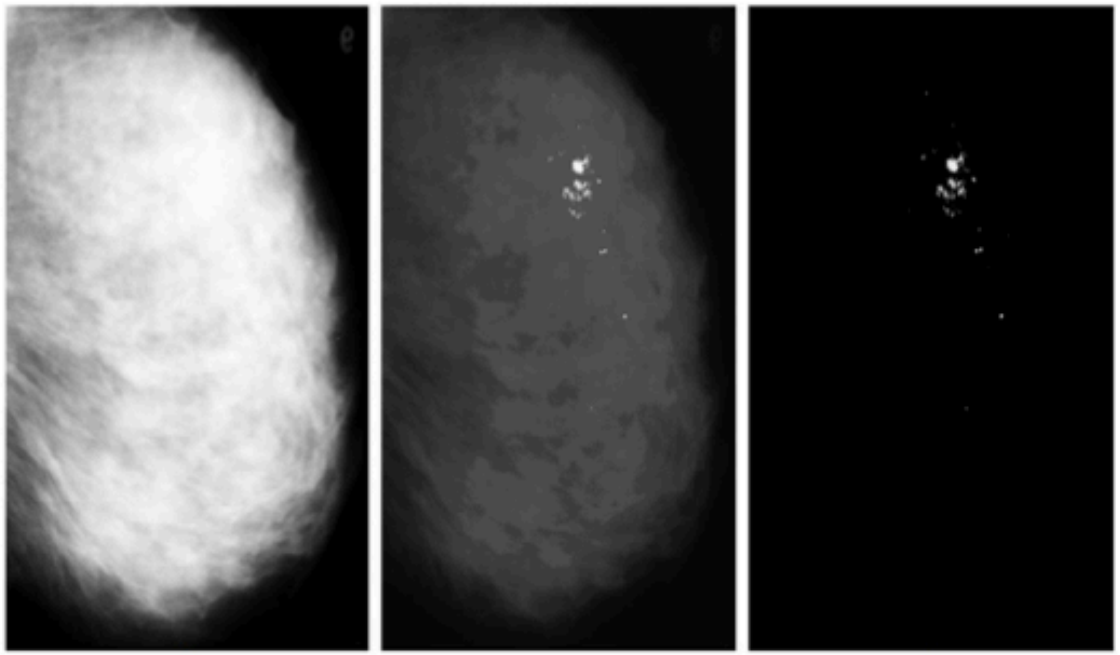

d e f

Brazilian Journal of Medical and Biological Research (2010) 43: 77-84
ISSN 0100-879X

Brain tissue segmentation using q-entropy in multiple sclerosis magnetic resonance images

P.R.B. Diniz[1], L.O. Murta-Junior[3], D.G. Brum[1], D.B. de Araújo[3] and A.C. Santos[1,2]

[1]Departamento de Neurociências e Ciências do Comportamento, [2]Departamento de Clínica Médica, Divisão de Radiologia, Faculdade de Medicina de Ribeirão Preto, Universidade de São Paulo, Ribeirão Preto, SP, Brasil
[3]Departamento de Física e Matemática, Faculdade de Filosofia, Ciências e Letras de Ribeirão Preto, Universidade de São Paulo, Ribeirão Preto, SP, Brasil

Abstract

The loss of brain volume has been used as a marker of tissue destruction and can be used as an index of the progression of neurodegenerative diseases, such as multiple sclerosis. In the present study, we tested a new method for tissue segmentation based on pixel intensity threshold using generalized Tsallis entropy to determine a statistical segmentation parameter for each single class of brain tissue. We compared the performance of this method using a range of different q parameters and found a different optimal q parameter for white matter, gray matter, and cerebrospinal fluid. Our results support the conclusion that the differences in structural correlations and scale invariant similarities present in each tissue class can be accessed by generalized Tsallis entropy, obtaining the intensity limits for these tissue class separations. In order to test this method, we used it for analysis of brain magnetic resonance images of 43 patients and 10 healthy controls matched for gender and age. The values found for the entropic q index were 0.2 for cerebrospinal fluid, 0.1 for white matter and 1.5 for gray matter. With this algorithm, we could detect an annual loss of 0.98% for the patients, in agreement with literature data. Thus, we can conclude that the entropy of Tsallis adds advantages to the process of automatic target segmentation of tissue classes, which had not been demonstrated previously.

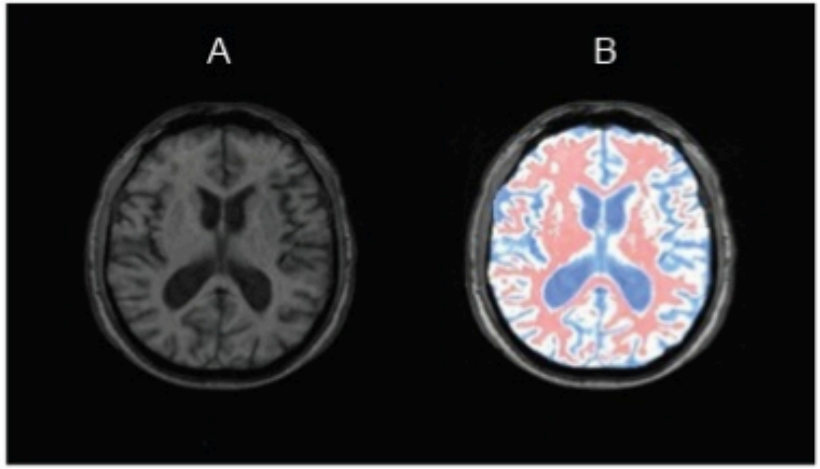

Figure 3. Maximum entropy segmentation example. *A*, Original image; *B*, image with the segmentation masks. Blue indicates cerebrospinal fluid, white indicates the gray matter, and red indicates the white matter.

The ideal q values for the segmentation of the classes are: CSF = 0.2, WM = 0.1, GM = 1.5, which have not been shown previously.

These characteristics allow its application to clinical routine.

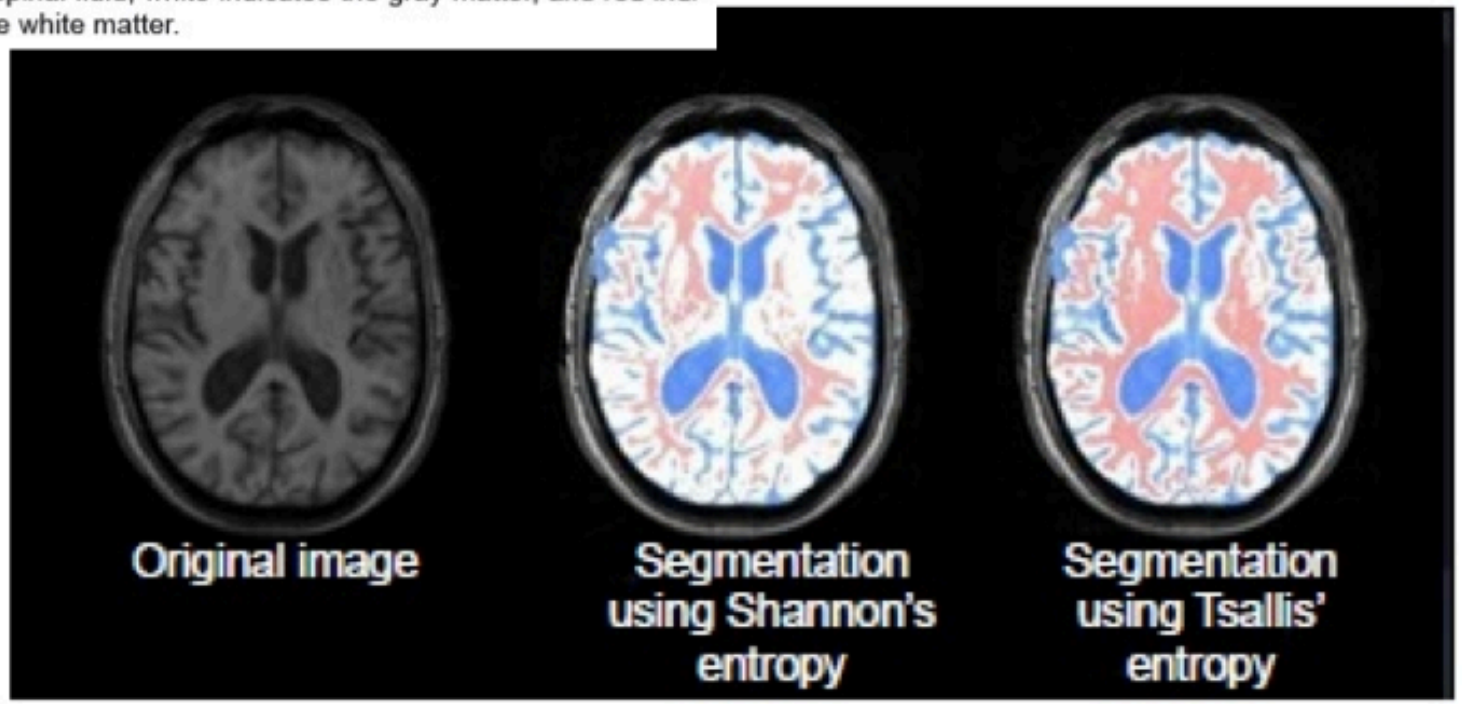

Figure 6. Segmentation using Shannon and Tsallis entropies.

PRB Diniz, LO Murta Jr., DG Brum, DB de Araujo and AC Santos
Braz. J. Med. Bio. Res. **43**, 77 (2010)

Weili SHI, Yanfang LI, Yu MIAO, Yinlong HU

Changchun University of Science and Technology

Research on the Key Technology of Image Guided Surgery

Abstract. *It research on the key technology on IGS (image-guided surgery). It proposes medical image segmentation based on PCNN and the virtual endoscopic scenes real-time rendering method based on GPU parallel computing technology, which improves the display quality of IGS's virtual scene and real-time rendering speed. These methods are very important for IGS's applications.*

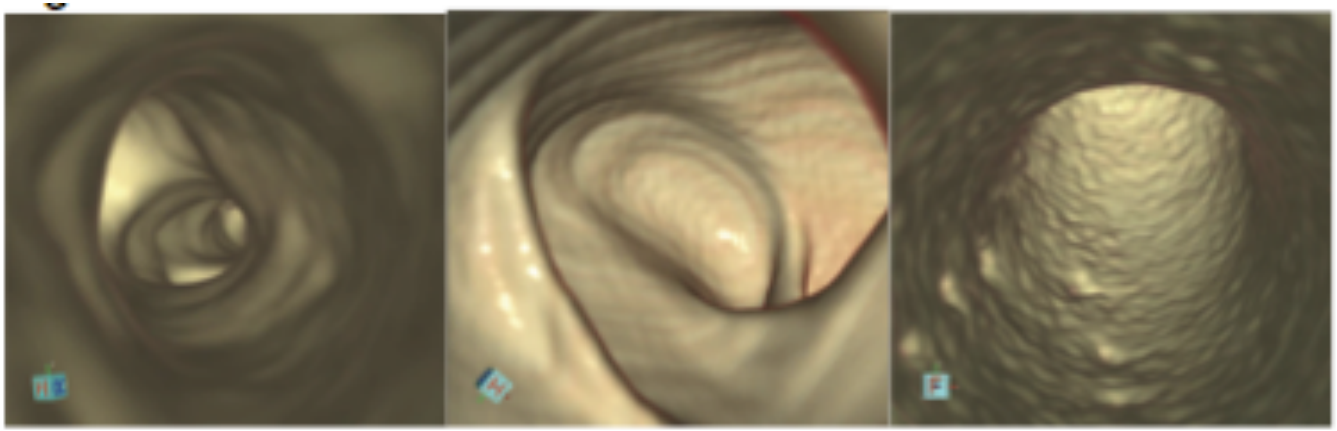

Fig.12. Bronchus Fig.13.Colon Fig.14.blood vessel

Table 1. Speed Comparison between Traditional Algorithms and Present Algorithm(uint: fps)

CT Image	Bronchus	Colon	blood vessel
Image Extent	512*51*217	512*512*252	512*512*355
Ray casting	9.8	6.4	3.5
Our algorithm	36.2	35.7	32.1

Tissue Radiation Response with Maximum Tsallis Entropy

O. Sotolongo-Grau* and D. Rodríguez-Pérez
UNED, Departamento de Física Matemática y de Fluidos, 28040 Madrid, Spain

J. C. Antoranz
UNED, Departamento de Física Matemática y de Fluidos, 28040 Madrid, Spain, and University of Havana, Cátedra de Sistemas Complejos Henri Poincaré, Havana 10400, Cuba

Oscar Sotolongo-Costa
University of Havana, Cátedra de Sistemas Complejos Henri Poincaré, Havana 10400, Cuba
(Received 22 June 2010; published 7 October 2010)

The expression of survival factors for radiation damaged cells is currently based on probabilistic assumptions and experimentally fitted for each tumor, radiation, and conditions. Here, we show how the simplest of these radiobiological models can be derived from the maximum entropy principle of the classical Boltzmann-Gibbs expression. We extend this derivation using the Tsallis entropy and a cutoff hypothesis, motivated by clinical observations. The obtained expression shows a remarkable agreement with the experimental data found in the literature.

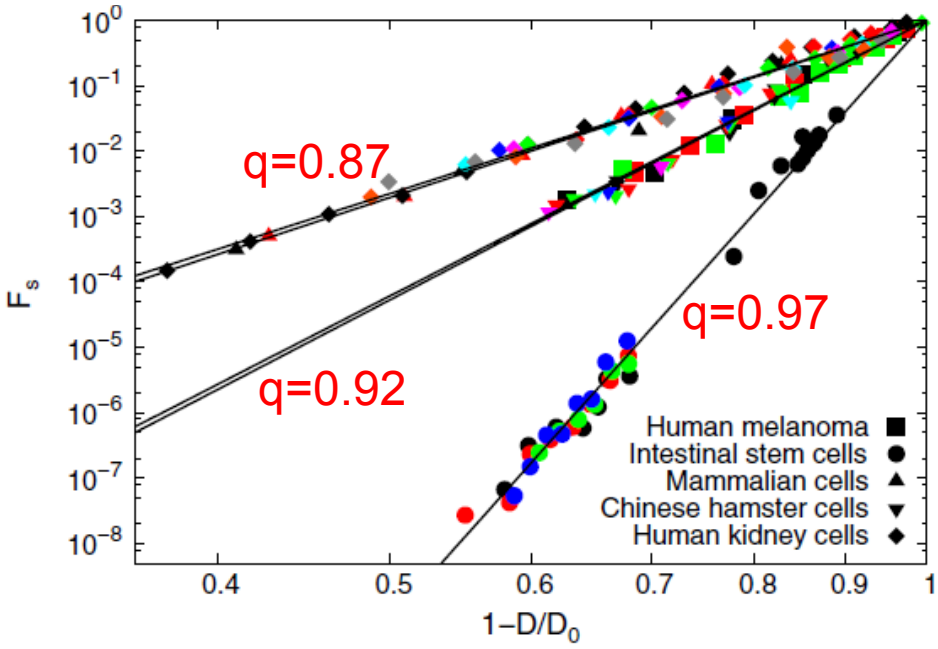

$$\gamma = \frac{2-q}{1-q}$$

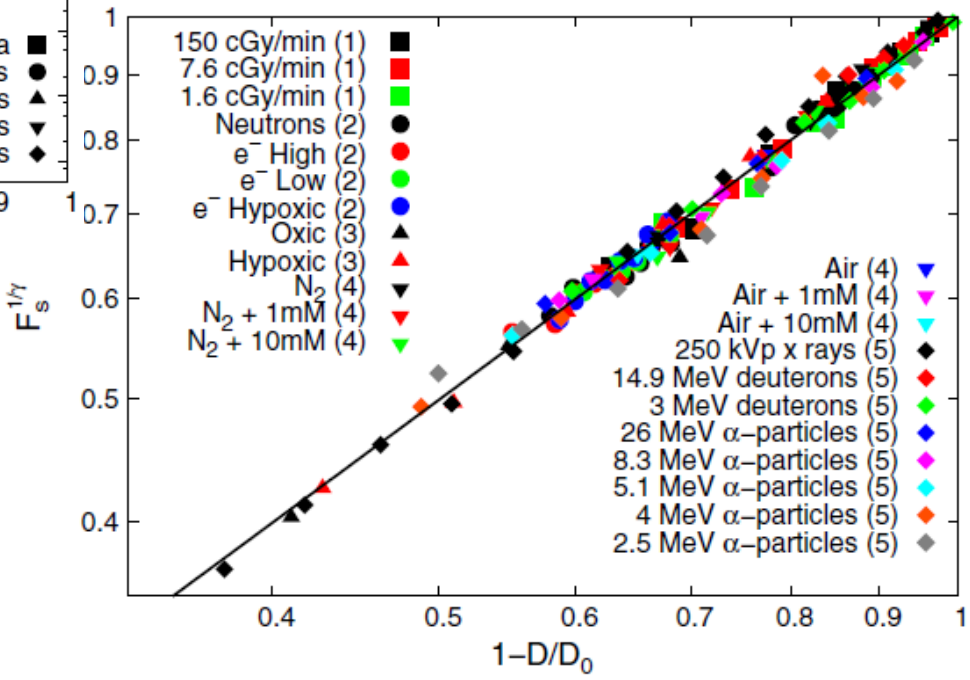

FIG. 2 (color online). Normalized survival fractions $(F_s)^{1/\gamma}$ as a function of the rescaled radiation dose, $1 - D/D_0$ for different tissues: intestinal stem cells (■), chinese hamster cells (●), human melanoma (▲), human kidney cells (▼), and cultured mammalian cells (◆) under different irradiation conditions detailed in [17–21] and grouped in [23]. The straight line shown is $y = x$.

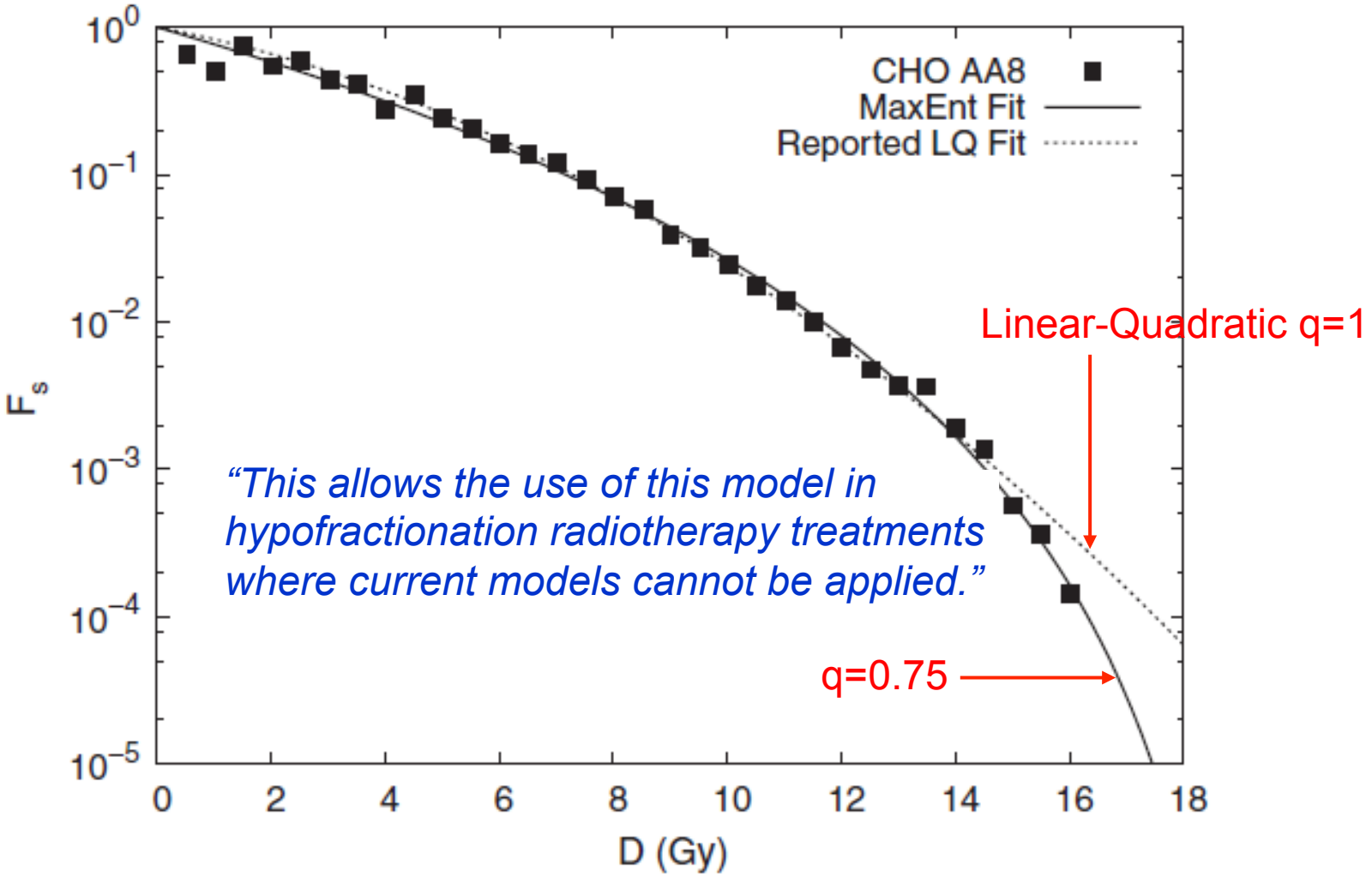

FIG. 3. Comparison between the LQ model best fit ($\alpha = 0.167 \pm 0.015$ Gy^{-1} and $\beta = 0.0205 \pm 0.0015$ Gy^{-2}) reported in [24] and our model fitted to $\gamma = 5.0 \pm 0.4$ and $D_0 = 19.4 \pm 0.4$ Gy for the cell line CHO AA8 under 250 k-Vp x rays.

Limoges - France

Journal of
Applied
Crystallography
ISSN 0021-8898

Strain-profile determination in ion-implanted single crystals using generalized simulated annealing

Alexandre Boulle[a]* and Aurélien Debelle[b]

Received 29 March 2010
Accepted 29 July 2010

[a]Science des Procédés Céramiques et de Traitements de Surface (SPCTS), CNRS UMR 6638, Centre Européen de la Céramique, 12 rue Atlantis, 87068 Limoges, France, and [b]Centre de Spectrométrie Nucléaire et de Spectrométrie de Masse (CSNSM, UMR 8609), CNRS – IN2P3 – Université Paris-Sud 11, Bâtiment 108, 91405 Orsay Cedex, France. Correspondence e-mail: alexandre.boulle@unilim.fr

A novel least-squares fitting procedure is presented that allows the retrieval of strain profiles in ion-implanted single crystals using high-resolution X-ray diffraction. The model is based on the dynamical theory of diffraction, including a B-spline-based description of the lattice strain. The fitting procedure relies on the generalized simulated annealing algorithm which, contrarily to most common least-squares fitting-based methods, allows the global minimum of the error function (the difference between the experimental and the calculated curves) to be found extremely quickly. It is shown that convergence can be achieved in a few hundred Monte Carlo steps, *i.e.* a few seconds. The method is model-independent and allows determination of the strain profile even without any 'guess' regarding its shape. This procedure is applied to the determination of strain profiles in Cs-implanted yttria-stabilized zirconia (YSZ). The strain and damage profiles of YSZ single crystals implanted at different ion fluences are analyzed and discussed.

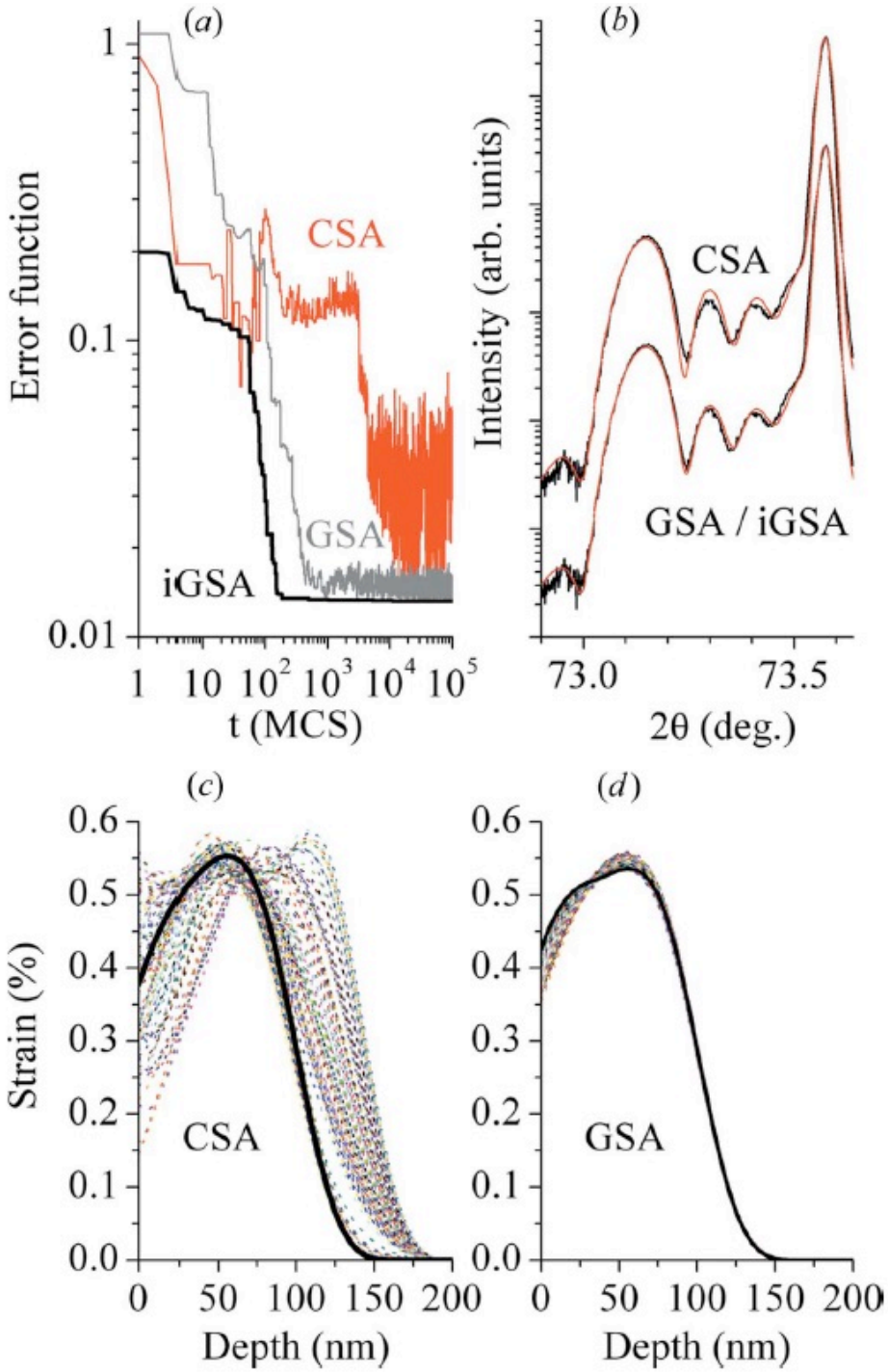
(a)
Error function
1
0.1
0.01
CSA
GSA
iGSA
1 10 10^2 10^3 10^4 10^5
t (MCS)
(b)
Intensity (arb. units)
CSA
GSA / iGSA
73.0
73.5
2θ (deg.)
(c)
Strain (%)
0.6
0.5
0.4
0.3
0.2
0.1
0.0
CSA
0 50 100 150 200
Depth (nm)
(d)
GSA
0 50 100 150 200
Depth (nm)

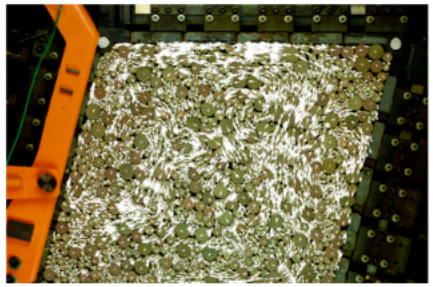

EDITORS' SUGGESTION

Experimental Validation of a Nonextensive Scaling Law in Confined Granular Media

The velocity distribution of sheared granular media shows unexpected similarities with turbulent fluid flows.

Gaël Combe, Vincent Richefeu, Marta Stasiak, and Allbens P.F. Atman

Phys. Rev. Lett. **115**, 238301 (2015)

Experimental Validation of a Nonextensive Scaling Law in Confined Granular Media

Gaël Combe,* Vincent Richefeu, and Marta Stasiak
Université Grenoble Alpes, 3SR, F-38000 Grenoble, France and CNRS, 3SR, F-38000 Grenoble, France

Allbens P. F. Atman†
Departamento de Física e Matemática, National Institute of Science and Technology for Complex Systems, Centro Federal de Educação Tecnológica de Minas Gerais – CEFET-MG, Avenida Amazonas 7675, 30510-000 Belo Horizonte-MG, Brazil

(Received 28 July 2015; published 1 December 2015)

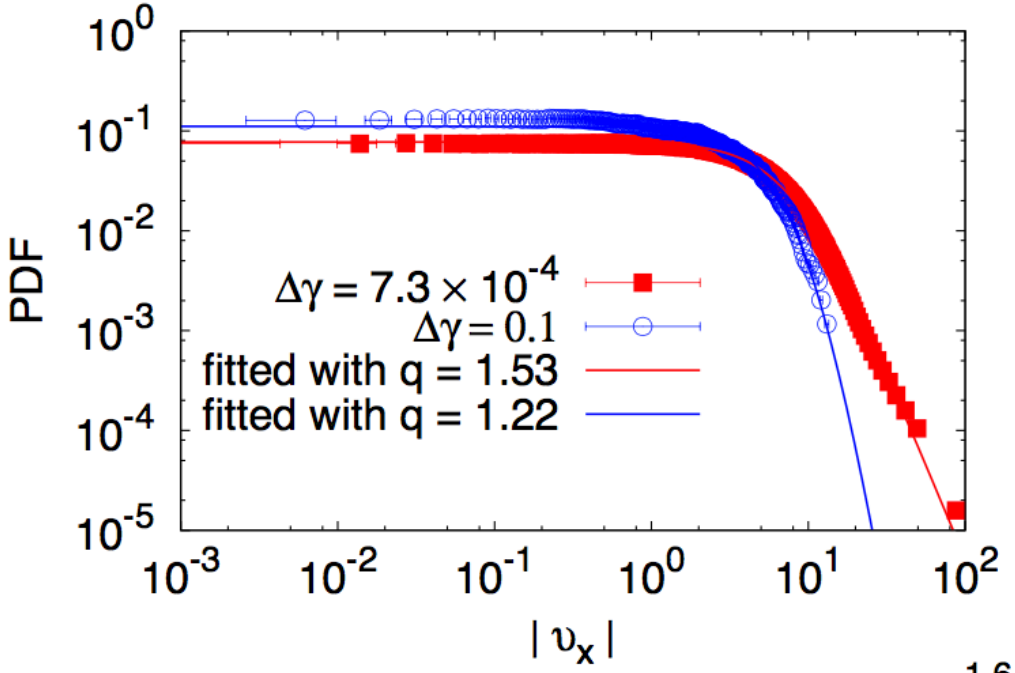

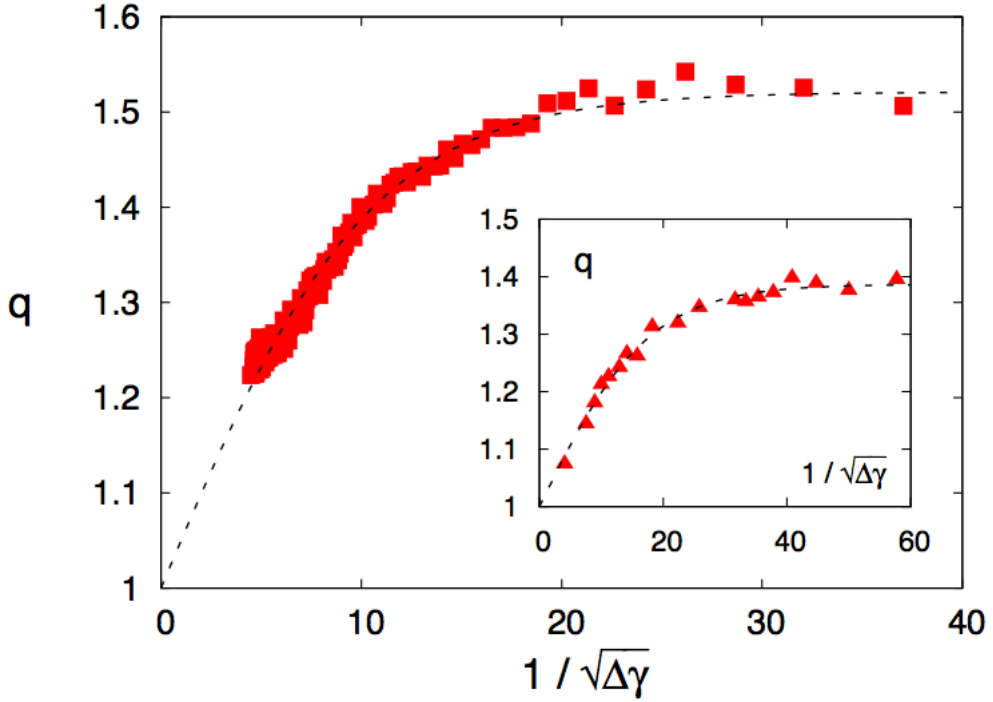

Combe, Richefeu, Stasiak and Atman
PRL **115**, 238301 (2015)

$$\langle x^2 \rangle \propto t^{\alpha}$$

Combe, Richefeu, Stasiak and Atman
PRL **115**, 238301 (2015)

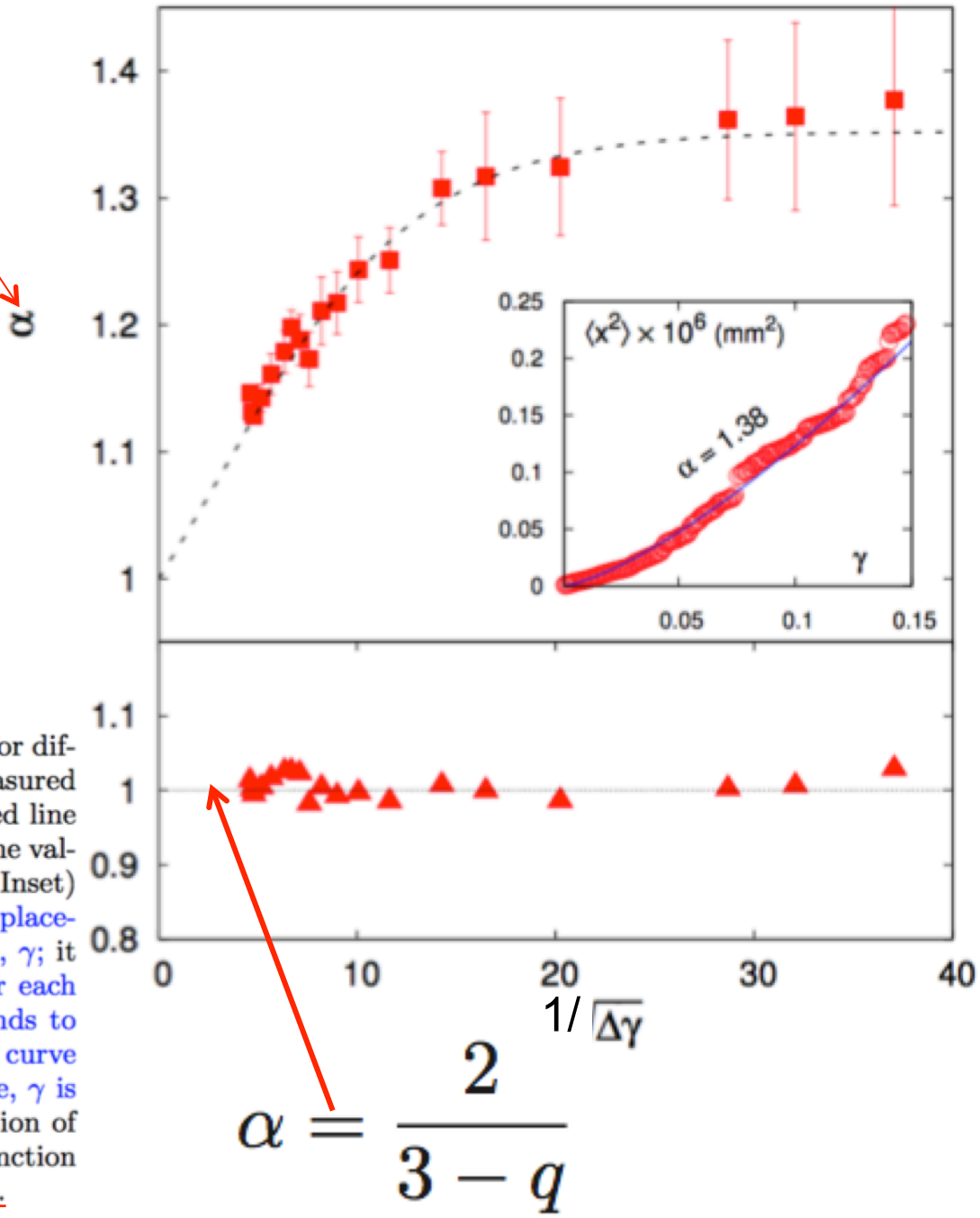

FIG. 4. Verification of the Tsallis-Bukman scaling law for different regimes of diffusion. (top) Evolution of the measured diffusion exponent α as a function of $1/\sqrt{\Delta\gamma}$ the dashed line is a direct application of the scaling law from the fit of the values shown in Fig. 3, $\alpha(1/\sqrt{\Delta\gamma}) = 2/[3 - q(1/\sqrt{\Delta\gamma})]$. (Inset) a typical diffusion curve showing the mean square displacement fluctuations, $\langle x^2 \rangle$, in function of the shear strain, γ; it allows the assessment of the diffusion exponent, α, for each strain window tested. In the case shown, it corresponds to the smallest strain window, the rightmost point in the curve at the main panel. Note that for a constant strain rate, γ is proportional to time. (Bottom) Measure of the deviation of the data relative to the scaling law prediction, as a function of $1/\sqrt{\Delta\gamma}$, showing an agreement on the order of $\pm 2\%$.

$$\alpha = \frac{2}{3 - q}$$

CT and DJ Bukman, PRE **54** (1996) R2197

A&A 539, A158 (2012)
DOI: 10.1051/0004-6361/201117767

Astronomy & Astrophysics

Nonextensive distributions of asteroid rotation periods and diameters

A. S. Betzler[1] and E. P. Borges[2]

[1] Programa de Engenharia Industrial, Escola Politécnica, Universidade Federal da Bahia, R. Aristides Novis 2, Federação, 40210-630 Salvador-BA, Brazil
e-mail: betzler.ssa@ftc.br
[2] Instituto de Física and National Institute of Science and Technology for Complex Systems, Universidade Federal da Bahia, Campus Universitário de Ondina, 40210-340 Salvador-BA, Brazil
e-mail: ernesto@ufba.br

Received 25 July 2011 / Accepted 5 December 2011

ABSTRACT

Context. We investigate the distribution of asteroid rotation periods from different regions of the solar system and diameter distributions of near-Earth asteroids (NEAs).
Aims. We aim to verify if nonextensive statistics satisfactorily describes the data.
Methods. Light curve data were taken from the Planetary Database System (PDS) with Rel ≥ 2. We also considered the taxonomic class and region of the solar system. Data of NEA were taken from the Minor Planet Center.
Results. The rotation periods of asteroids follow a q-Gaussian with $q = 2.6$ regardless of taxonomy, diameter, or region of the solar system of the object. The distribution of rotation periods is influenced by observational bias. The diameters of NEAs are described by a q-exponential with $q = 1.3$. According to this distribution, there are expected to be 994 ± 30 NEAs with diameters greater than 1 km.

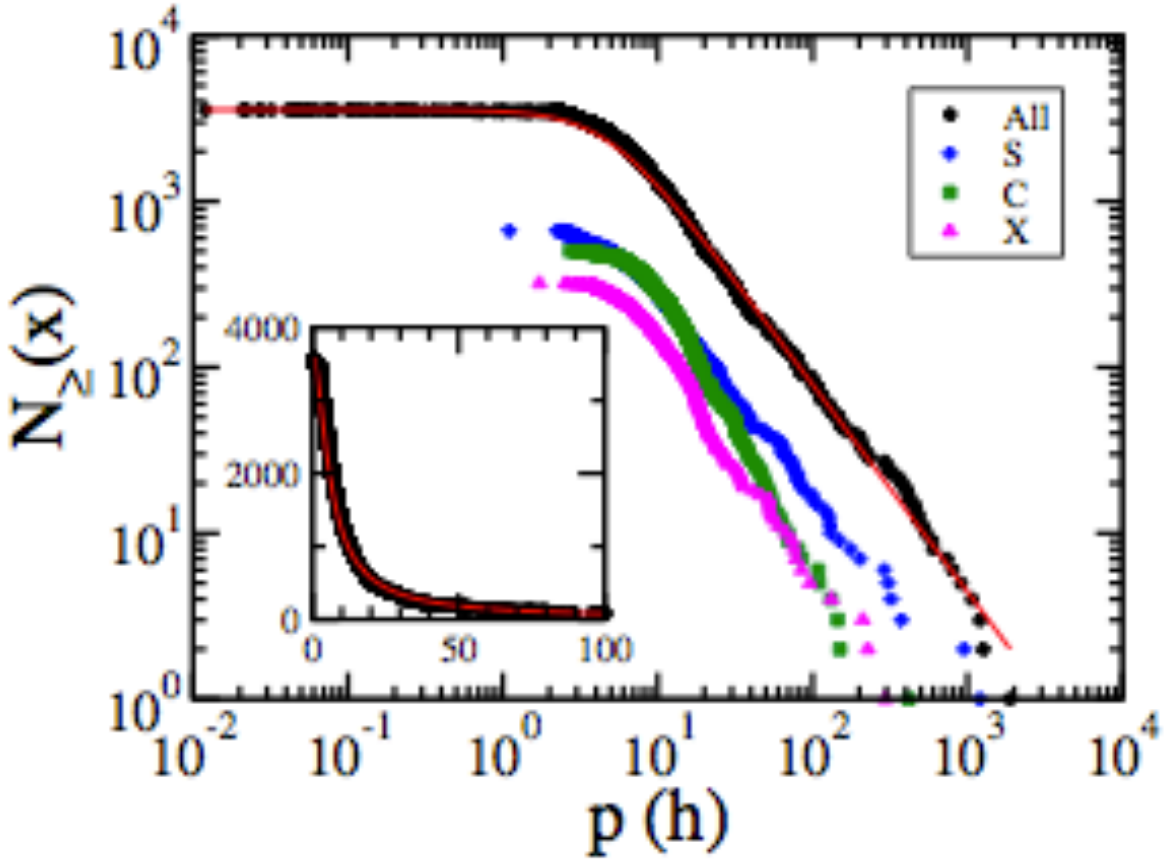

Fig. 3. Log-log plot of the decreasing cumulative distribution of periods of 3567 asteroids (dots) with Rel $\geq$ 2 taken from the PDS (NASA) and a q-Gaussian distribution ($N_{\geq}(p) = M \exp_q(-\beta_q p^2)$) (solid line), with $q = 2.6$, $\beta_q = 0.025$ h^{-2}, $M = 3567$. The other curves are 663 S-complex asteroids (diamonds, blue online), 503 C-complex asteroids (squares, green online), 321 X-complex asteroids (triangles, magenta online). Inset shows the 3567 asteroids and the q-Gaussian in a linear-linear plot.

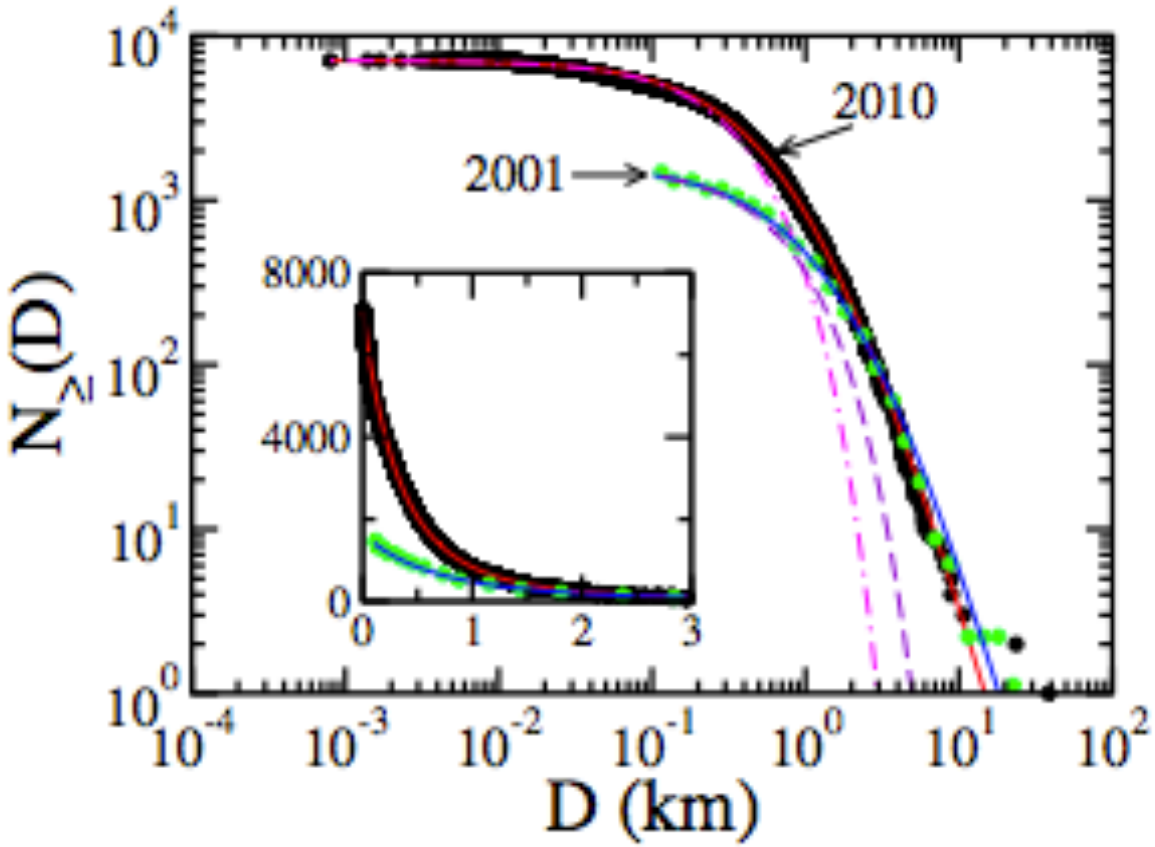

Fig. 4. Decreasing cumulative distribution of diameters of known NEAs in 2001 (1649 objects, green dots) and in 2010 (7078 objects, black dots). Solid lines are best fits of q-exponentials ($N_{\geq}(D) = M \exp_q(-\beta_q D)$). Blue line (2001): $q = 1.3$, $\beta_q = 1.5$ km^{-1}, $M = 1649$, red line (2010): $q = 1.3$, $\beta_q = 3$ km^{-1}, $M = 7078$. Normal exponentials ($q = 1$) are displayed in the main panel for comparison (dashed violet, with $\beta_1 = 1.5$ km^{-1}, $M = 1649$, and dot-dashed magenta, with $\beta_1 = 3$ km^{-1}, $M = 7078$).

Hydra viridissima:

A Upadhyaya, J-P Rieu, JA Glazier and Y Sawada, Physica A **293**, 549 (2001)

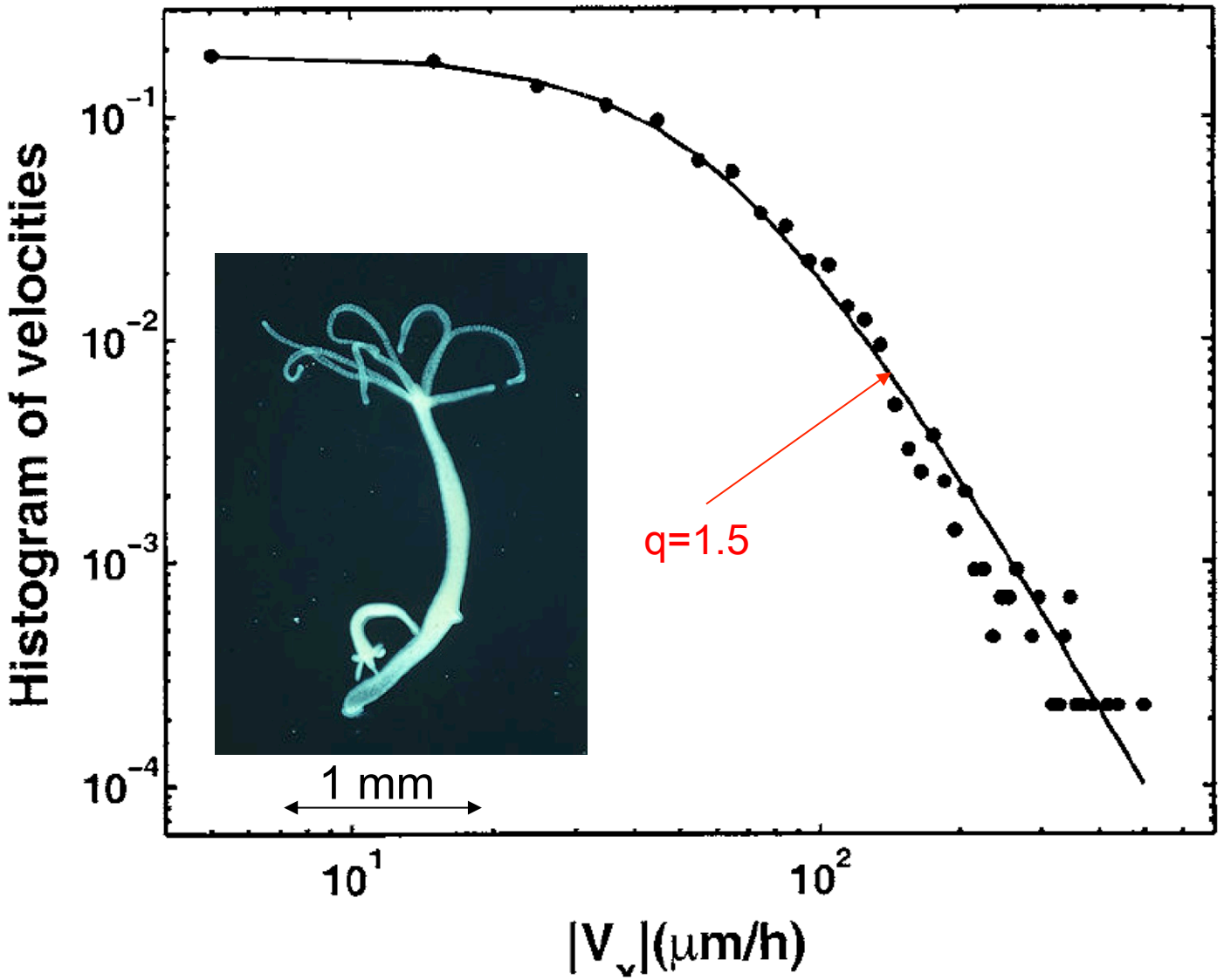

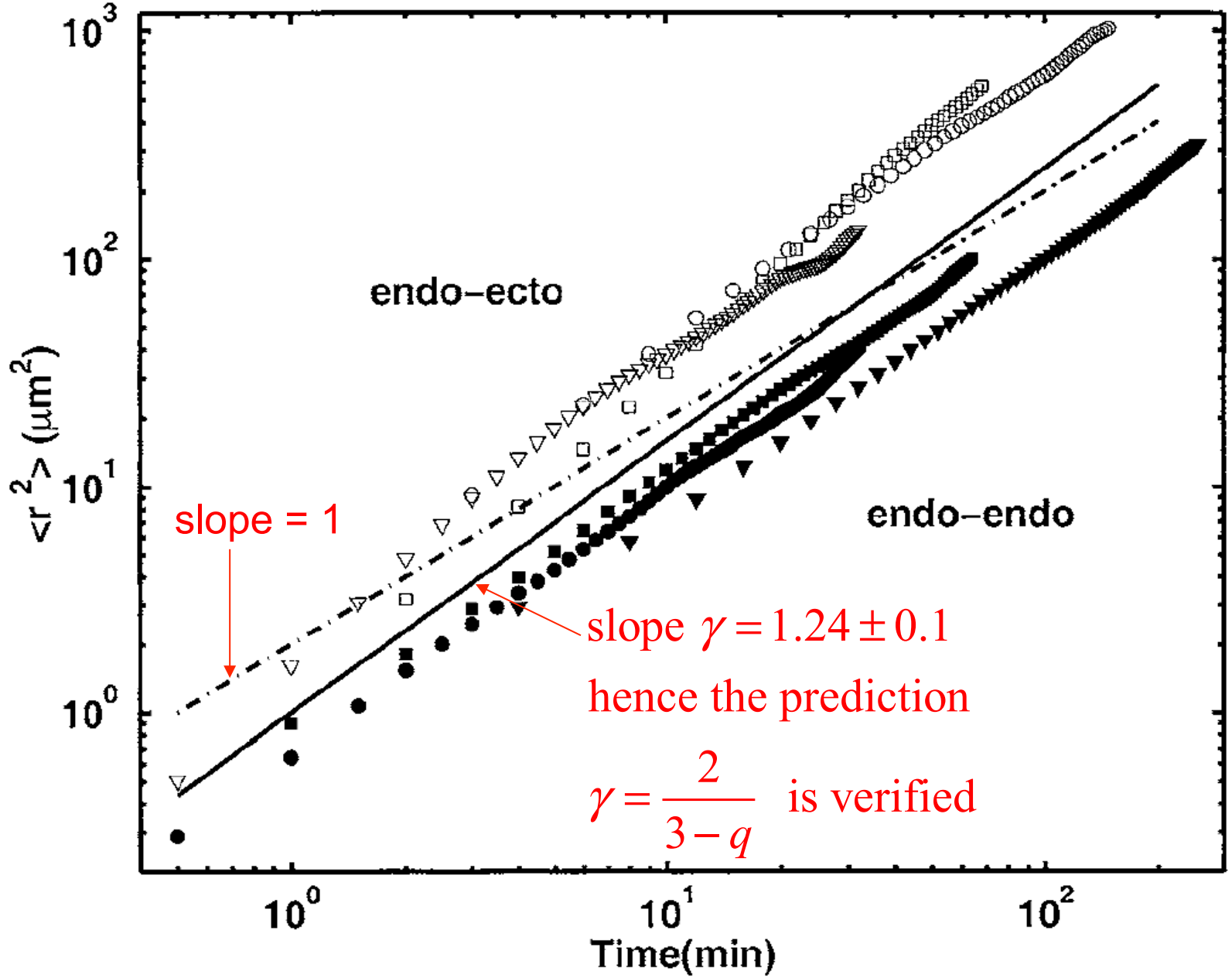

A Upadhyaya, J-P Rieu, JA Glazier and Y Sawada, Physica A **293**, 549 (2001)

Dictyostelium discoideum (cells):

A.M. Reynolds, Physica A **389**, 273 (2010)

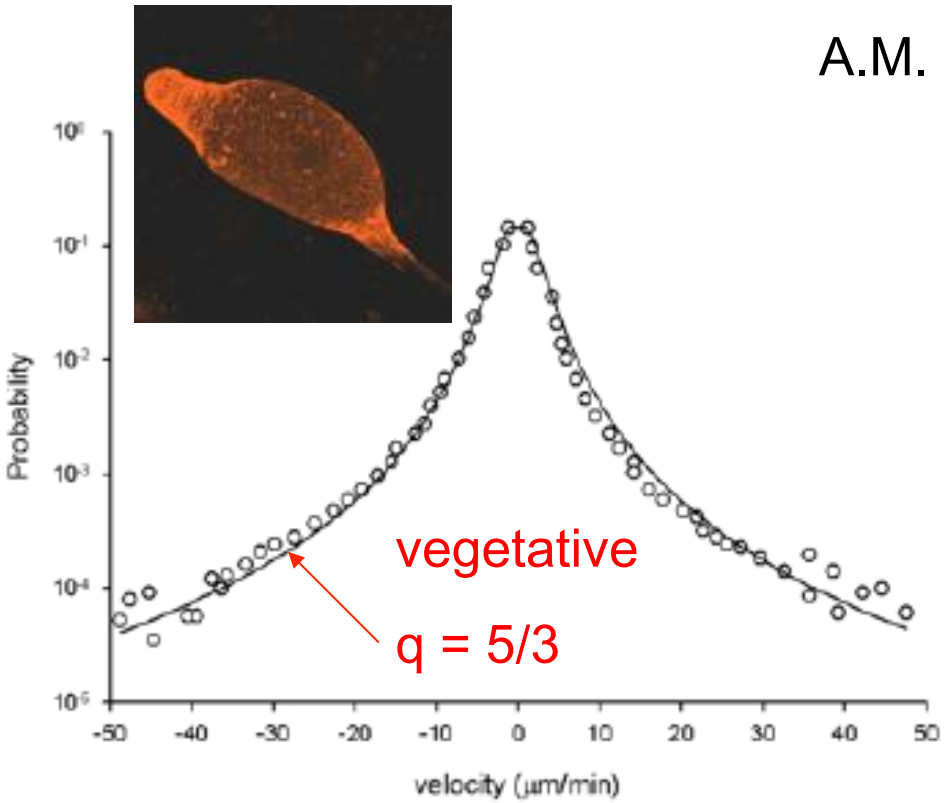

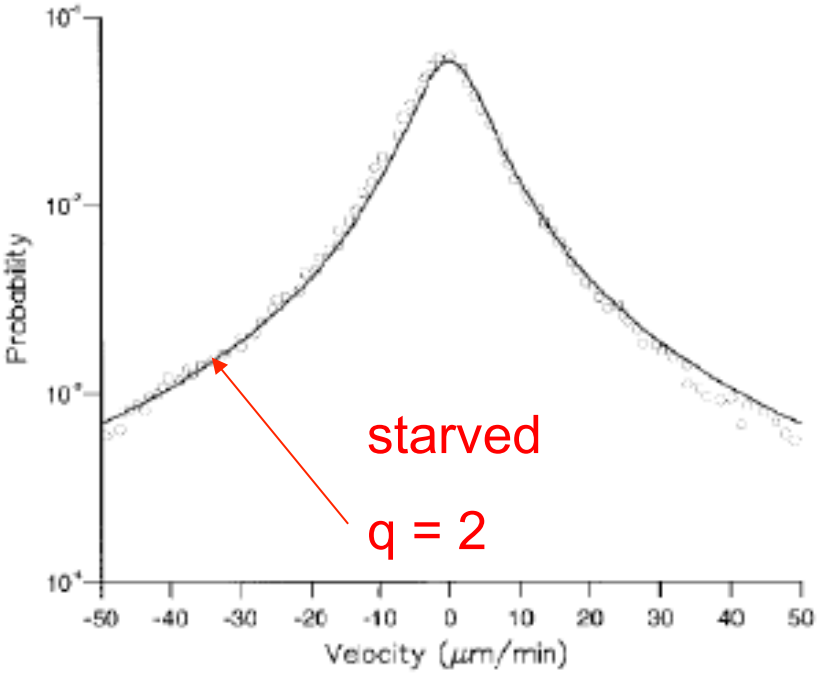

$$P(v) = \frac{\Gamma\left(\frac{\alpha+1}{2}\right)}{\sqrt{\pi}\ \Gamma\left(\frac{\alpha}{2}\right)} \frac{v_a^{\alpha}}{\left[v_a^2 + v^2\right]^{\frac{\alpha+1}{2}}} \equiv \frac{P(0)}{\left[1+(q-1)\ \beta\ v^2\right]^{\frac{1}{q-1}}}$$

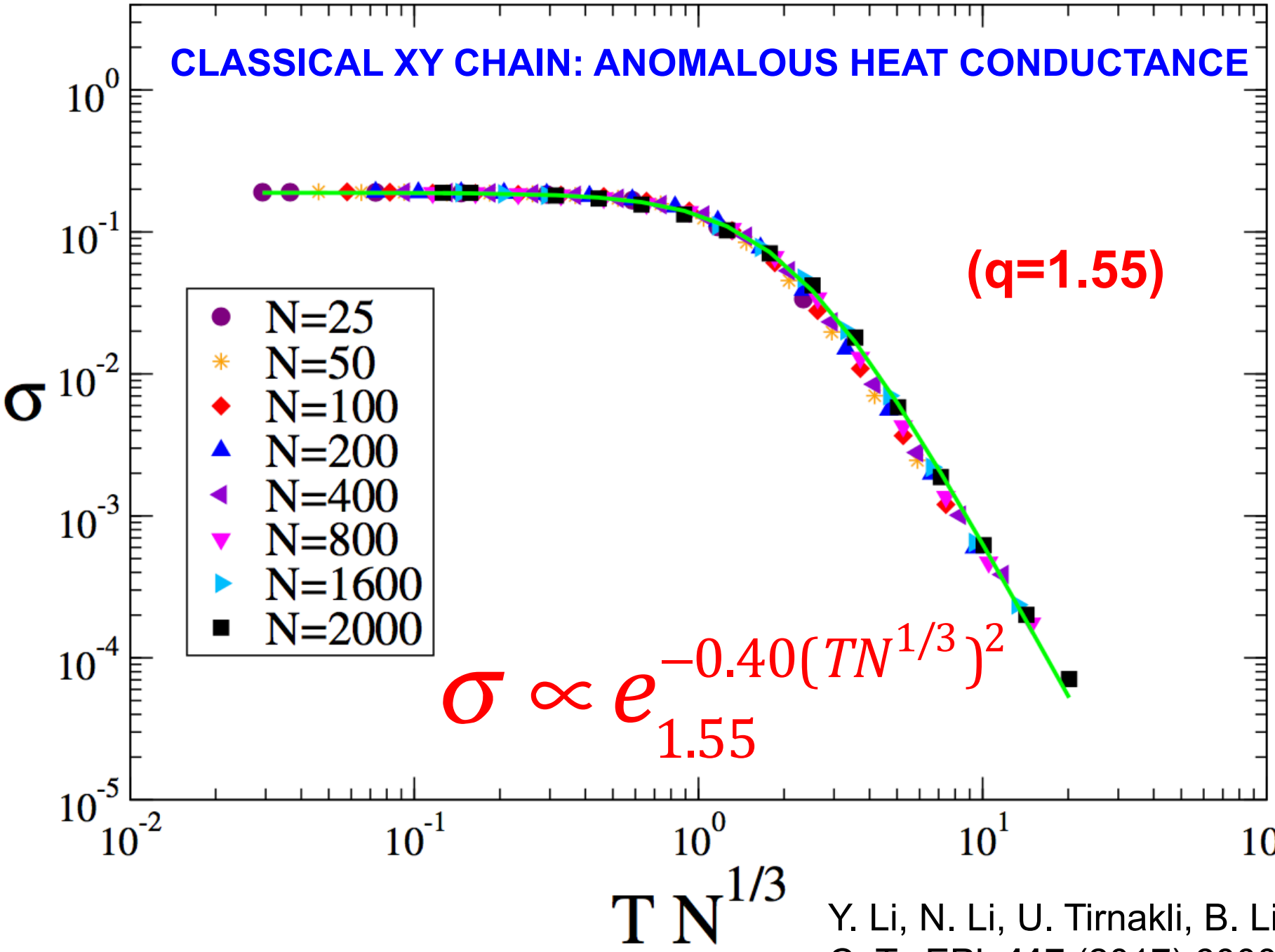

Y. Li, N. Li, U. Tirnakli, B. Li ar
C. T., EPL **117** (2017) 60004

Networks

AN ANALYTICALLY SOLVABLE MODEL:

R. Albert and A.-L. Barabasi, Phys. Rev. Lett. **85**, 5234 (2000)

At each time step,

m *new links are added with probability* p,

or m *existing links are rewired with probability* r,

or a new node with m *links is added with probability* $1 - p - r$

$$degree\ distribution \equiv p(k) \propto e_q^{-k/\kappa}$$

with

$$q = \frac{2m(2-r)+1-p-r}{m(3-2r)+1-p-r}$$

$$\left[written\ in\ the\ form\ \ p(k) \propto \frac{1}{(k+k_0)^{\gamma}}\ by\ the\ authors \right]$$

GEOGRAPHIC PREFERENTIAL ATTACHMENT GROWING NETWORK:

THE NATAL MODEL

D.J.B. Soares, C. T. , A.M. Mariz and L.R. Silva, Europhys Lett **70**, 70 (2005)

(1) Locate site i=1 at the origin of say a plane

(2) Then locate the next site with

$$P_G \propto 1/r^{2+\alpha_G} \quad (\alpha_G \geq 0)$$

$(r \equiv \textit{distance to the baricenter of the pre-existing cluster})$

(3) Then link it to only one of the previous sites using

$$p_A \propto k_i / r_i^{\alpha_A} \quad (\alpha_A \geq 0)$$

$(k_i \equiv \textit{links already attached to site } i)$

$(r_i \equiv \textit{distance to site } i)$

4) Repeat

$$(\alpha_{\mathrm{G}} = 1; \alpha_{A} = 1; N = 250)$$

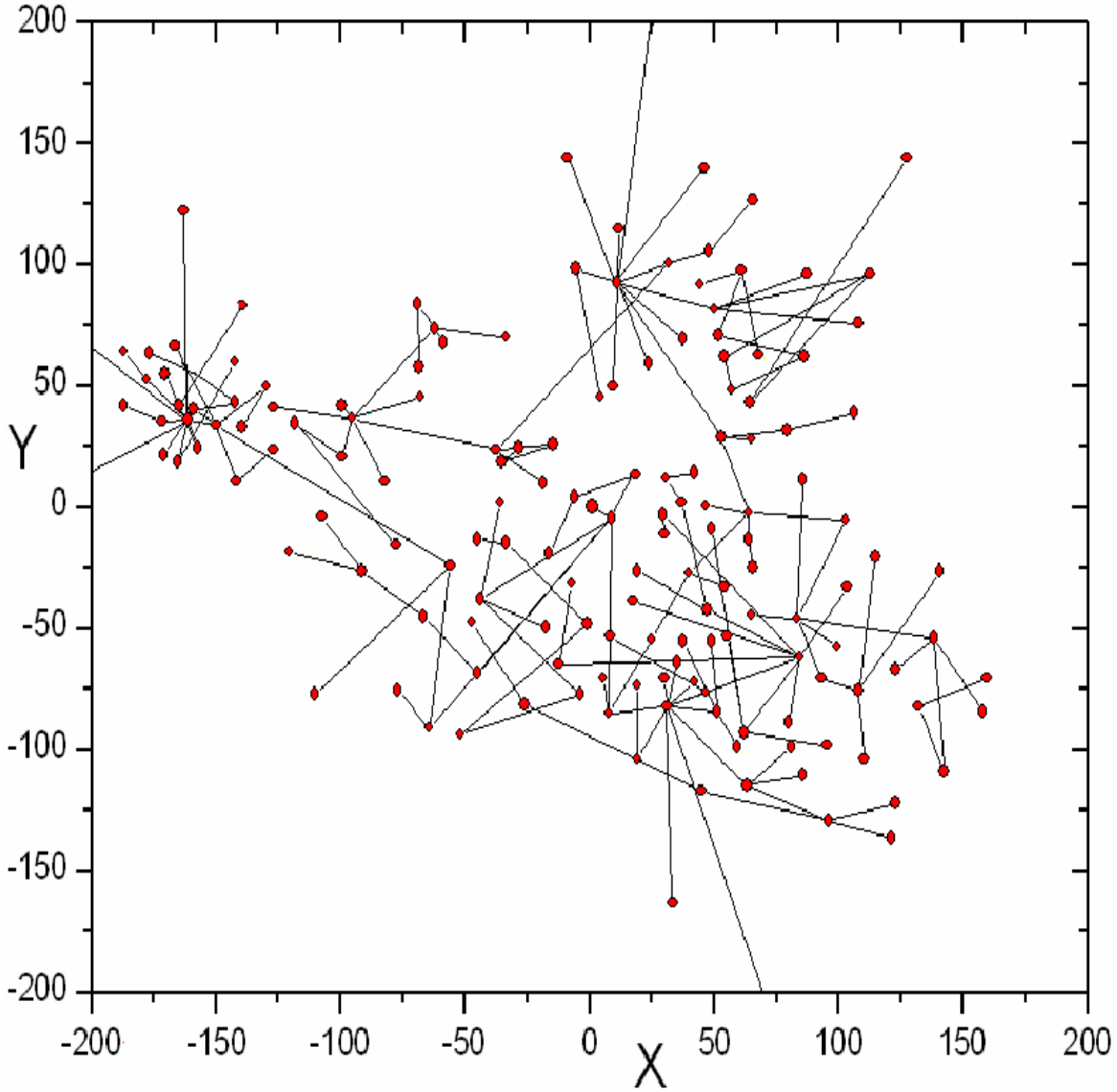

D.J.B. Soares, C. T. , A.M. Mariz and L.R. Silva, Europhys Lett **70**, 70 (2005)